HHS Public Access

Author manuscript

Gene Ther. Author manuscript; available in PMC 2022 August 20.

Published in final edited form as:

Gene Ther. 2022 August ; 29(7-8): 418–424. doi:10.1038/s41434-021-00275-5.

rAAV-based and intraprostatically delivered miR-34a therapeutics for efficient inhibition of prostate cancer progression

Jianzhong Ai[1,2,✉], **Jia Li**[2], **Qin Su**[2], **Hong Ma**[2], **Ran He**[2], **Qiang Wei**[1], **Hong Li**[1], **Guangping Gao**[2,✉]

[1]Department of Urology, Institute of Urology, West China Hospital, Sichuan University, Chengdu, China.

[2]Horae Gene Therapy Center, University of Massachusetts Medical School, Worcester, MA, USA.

Abstract

At present, there is no effective treatment for prostate cancer (PCa). Previous studies have reported that miR-34a is significantly downregulated in PCa cells; therefore, modulation of miR-34a expression might be a promising therapeutic approach for PCa treatment. To this end, we first verified the downregulation of miR-34a in prostate tumors from a transgenic adenocarcinoma mouse prostate (TRAMP) model. We found that miR-34a overexpression significantly inhibited the cell cycle, viability, and migration of PCa cells by targeting its downstream genes. Next, we tested the concept of intraprostatic injection of rAAV9·pri-miR-34a into 8-week-old TRAMP mice to inhibit PCa progression. We observed that the treatment lowered body weights significantly compared to the control treatment starting at 30 weeks after injection. rAAV9·pri-miR-34a treatment also obviously extended the lifespan of TRAMP mice. Moreover, we confirmed that the neoplasia in the treated prostates was significantly diminished compared to that in the control group. In addition, overexpressed miR-34a downregulated the expression of its target genes. Taken together, our results demonstrated, for the first time, the potential of rAAV-mediated efficient modulation of miR-34a expression in the prostate to inhibit PCa progression by regulating its downstream gene expression.

INTRODUCTION

Prostate cancer (PCa) is the second most commonly diagnosed cancer and the fifth leading cause of cancer-related mortality for males worldwide [1]. In the USA, PCa is the malignancy with the highest incidence and the second highest death rate [2].

✉**Correspondence** and requests for materials should be addressed to J.A. or G.G. jianzhong.ai@wchscu.cn; guangping.gao@umassmed.edu.

COMPETING INTERESTS

GG is a co-founder of Voyager, Adrenas, and AspA Therapeutics specialized in rAAV-based gene therapy, and holds equity in the companies. GG is an inventor on patents with potential royalties licensed to Voyager, AspA, and other biopharmaceutical companies.

The progression of PCa seriously affects male urinary and sexual functions, e.g., urinary retention and erectile dysfunction, which can dramatically reduce the quality of life of patients [3]. Advanced metastatic PCa is accompanied by the metastasis of bone, lung, lymph nodes, and other tissues and organs, which causes severe pain and dyspnea [4–6]. For patients with PCa at different stages, multiple approaches are currently used for effective treatment, including radical prostatectomy, local deep freezing, androgen deprivation therapy, and chemotherapy [7, 8]. In the past decade, immunotherapy (sipuleucel-T) [9], abiraterone, and enzalutamide [10, 11] have shed light on the therapeutics of PCa, especially for patients with advanced metastatic PCa. However, tumor recurrence is still a main challenge for PCa patients. Therefore, it is meaningful to explore an alternative approach for the effective treatment of PCa.

Recently, noncoding RNAs, including microRNAs (miRNAs), circular RNAs, and long intergenic RNAs, have been reported to play critical roles in tumorigenesis by regulating oncogene or tumor repressor gene expression [12–14]. Among them, miR-34a has been widely studied in various carcinomas, including lung cancer, colon cancer, and pancreatic cancer [15–17]. In PCa, previous studies demonstrated that miR-34a expression was significantly downregulated, and its role was also investigated [18].

To further explore the therapeutic role of miR-34a in PCa progression in vivo, recombinant adeno-associated virus (rAAV) was used to deliver miR-34a into the mouse prostate. Recently, rAAV was deemed a powerful tool for gene therapy due to its advantages of long-term expression, low immunogenicity, and nonchromosomal integration [19], and an rAAV-based drug for Leber congenital amaurosis, type 2 (LCA2) was approved by the U.S. Food and Drug Administration in 2017 [20], indicating an attractive prospect of rAAV-based gene therapy for various diseases. As reported previously, we mapped the transduction profile of 12 serotypes of rAAV in vivo and in vitro [21], and we found that rAAV9 was a promising vector for transducing genes or miRNAs in prostate tissue or PCa cells.

In this study, we aimed to comprehensively evaluate the effect of rAAV9-delivered miR-34a on PCa progression in vitro and in vivo and to test the therapeutic potential of rAAV for effective and safe delivery of miRNA therapeutics. These results will pave the way for the effective treatment of PCa.

METHODS

Cells and TRAMP mouse model

PC3 (CRL-1435) and TRAMP-C2 (CRL-2731) cells were purchased from ATCC (Manassas, VA, USA), and they were cultured with F-12K medium and DMEM, respectively, supplemented with 10% fetal bovine serum (FBS) and 1% ampicillin/streptomycin in a humidified atmosphere of 5% CO_2 at 37 °C. The 293 cells were maintained in our lab and cultured with DMEM. The transgenic adenocarcinoma of the mouse prostate (TRAMP) mouse model was obtained from JAX lab [22, 23], and the animals were maintained and used as per the guidelines of the Institutional Animal Care and Use Committee (IACUC) of the University of Massachusetts Medical School. All animals were randomly and blindly divided into each group.

rAAV production and titration

rAAV vectors were produced using the standard triple transfection method as described previously [24]. Viruses were purified by ultracentrifugation over cesium chloride (CsCl) and titrated by both silver staining and quantitative polymerase chain reaction (qPCR). Two different viral preparations were tested for each serotype [19].

Intraprostatic and intratumoral injection of TRAMP mice

The 8-week-old mice were anesthetized with isoflurane, and the abdominal cavity was opened to expose the prostate gland. Then, 1×10^{11} genome copy (GC) of the rAAV vector diluted in 10 μL of sterile PBS was injected into each of two sites of the anterior prostate (AP) and two sites of the dorsal lateral prostate (DLP). After injection, the abdominal cavity was sutured. Prostates were harvested 4 weeks after intraprostatic injection under a dissection microscope. Moreover, 3×10^6 TRAMP-C2 cells in 100 μL of PBS were injected into the right flanks of C57/B6 mice, and 1×10^{11} GC of rAAV vector was injected into tumors that were ~100 mm^3 in size. Next, tumor tissues were harvested after 7 days of injection. All animal study protocols were approved by the University of Massachusetts Medical School IACUC.

Real-time quantitative PCR for miRNA and mRNA detection

RNA extraction and real-time qPCR for miRNA (TaqMan miRNA assay; miR-34a; Life Technologies, Carlsbad, CA, USA) and mRNAs were performed as described previously [25]. Primer sequences for CCND1, TOP2A, and CD44 are listed in Table 1. U6 and β-actin were used as internal controls for miRNAs and mRNAs, respectively.

Reporter gene assay

The targeting efficacy of miR-34a was confirmed using a reporter gene assay. Briefly, the sequence of 3× miR-34a binding sites was cloned downstream of the β-galactosidase gene z (LacZ) gene open reading frame in the pmiCHECK expressing both LacZ and firefly luciferase (Fluc). The plasmid pAAVsc CB PI-miR-34a-Gluc was constructed by inserting the sequence of pri-miR-34a into the multiple cloning site. Then, the plasmids were transfected into 293 cells for 48 h, and the activities of LacZ and Fluc were measured using kits from Thermo Fisher (T2265, Waltham, MA) and Promega (E1500, Madison, WI), respectively.

Cell cycle analysis

The cell cycle was analyzed using FxCycl PI/RNase Staining Solution from Life Technologies (Carlsbad, CA, USA). Cells were harvested and fixed with 70% ethanol at 4 °C overnight; then cells were washed and stained with 0.5 mL of FxCycle PI/RNase Staining Solution for 30 min at room temperature in the dark. Finally, the cell cycle was measured using a flow cytometer (Guava EasyCyte HT, EMD Millipore, Billerica, MA, USA), and the data were analyzed using Flow Jo software (FLOWJO, Ashland OR, USA).

Cell Counting Kit 8 (CCK8) assay

The CCK8 reagent was purchased from Abcam (ab228554, Cambridge, MA, USA). Briefly, cells were seeded into a 96-well plate at a concentration of 5000 cells per well, and the cells were transfected with plasmids expressing green fluorescence protein and miR-34a for 48 h. Then, the cells were incubated with 10 μL of CCK8 solution for 75 min at 37 °C in the dark. Finally, the absorbance was measured at 460 nm.

Wound healing assay

PC3 cells were seeded into a six-well plate at a density of 5×10^5 cells/well, and the cells were transfected with plasmids of AAV-miR-34a for 48 h. Next, the cell monolayer was scratched using a 10-μL tip. The wound width was recorded using a microscope and further analyzed by ImageJ software.

Western blotting

Total proteins were extracted from cultured cells and mouse prostate tissues using radioimmunoprecipitation assay buffer supplemented with protease and phosphatase inhibitors (Thermo Fisher Scientific, Waltham, MA, USA). In total, 15 μg of protein was separated in a 4–20% gradient SDS-polyacrylamide gel and transferred onto nitrocellulose membranes (Bio-Rad Laboratories, Hercules, CA, USA). Nonspecific binding was blocked with 5% nonfat milk in Tris-buffered saline with Tween 20 as recommended for each antibody. The membranes were further incubated with rabbit anti-Sox4 (ab86809; Abcam, Cambridge, MA, USA), anti-Aldoa (ab232786; Abcam), anti-Ccnd1 (ab16663; Abcam), mouse anti-E-cadherin (Cat. no. 202183; ZEN BIO, Chengdu, China), and rabbit anti-CCND1 (Cat. no. 382442; ZEN BIO) antibodies overnight at 4 °C. IRDye 800CW goat anti-rabbit IgG (Cat. no. 926–32211; LI-COR, Lincoln, NE, USA), goat anti-IgG (H + L chain) (mouse) pAb-HRP (Cat. No. 330, MBL, Beijing, China), and goat anti-IgG (H + L chain) (rabbit) pAb-HRP (Cat. No. 458, MBL) were used as the secondary antibodies, while rabbit anti-beta-actin (ab8227; Abcam) and mouse anti-β-tubulin (Cat. no. 200608; ZEN BIO) were used as internal controls.

Immunofluorescence staining and histological analysis

As described previously [26], mouse prostates and tumor tissues were fixed in 10% buffered formalin overnight at 4 °C and then sequentially dehydrated in 10–30% sucrose at 4 °C. The samples were embedded in optimal cutting temperature compound (Sakura Finetek, Torrance CA, USA) and stored at −80 °C. Eight micron-thick cryosections were obtained and washed three times with 1× PBS for 5 min each. Next, the sections were mounted with VECTASHIELD mounting medium containing DAPI (Vector Laboratories, Burlingame CA, USA). For HE staining, the prostate tissues were fixed in 10% buffered formalin overnight at RT, embedded in paraffin and sectioned to 4-micron thickness. Sections were stained with hematoxylin and eosin and imaged using a bright field microscope (Leica, Buffalo Grove IL, USA).

Alanine aminotransferase (ALT) and aspartate aminotransferase (AST) detection

Blood was collected by facial vein bleeding before and at 2 and 4 weeks after intraprostatic injection, and serum was separated using a Microtainer tube with a serum separator (Cat. no. #365967) from BD (Franklin Lakes, NJ, USA). AST and ALT levels were analyzed using an AST colorimetric endpoint kit (Cat. no. #A561) and an ALT colorimetric endpoint kit (Cat. no. #A526) from TECO Diagnostics (Anaheim, CA, USA), respectively, as per the instructions.

rAAV GC number

Tissues were harvested and stored in RNAlater solution (Life Tech, Carlsbad, CA). Total DNA was extracted using the AllPrep DNA/RNA Mini Kit (Qiagen, Hilden, Germany) according to the manufacturer's instructions. Multiplexed droplet digital PCR (ddPCR) was performed by a QX200 ddPCR system (Bio-Rad) using TaqMan primers and probes targeting EGFP (Mr00660654_cn, Life Tech) and the reference gene transferrin receptor (Tfrc) (4458367, Life Tech). rAAV GC numbers per diploid genome were calculated by dividing EGFP transgene copy numbers by two Tfrc gene copies.

Statistical analysis

The experiments were performed in triplicate, and all data are presented as the means ± standard error of the mean or means ± the standard deviation. Statistical significance for comparisons among multiple groups (≥3) and between two groups was determined using analysis of variance and Student's paired *t* test, respectively, in GraphPad Prism 7.0.

RESULTS

Downregulation of miR-34a along with PCa progression

To confirm the downregulation of miR-34a, our study first detected its expression in tumor tissue of TRAMP mice. The qPCR data showed that miR-34a expression was decreased significantly in the AP and DLP of TRAMP mice with respect to WT mice (Fig. 1A). Furthermore, we analyzed miR-34a expression in mouse prostate at different stages of PCa, and the results indicated that the expression of miR-34a in prostatic intraepithelial neoplasia (PIN) and tumor tissues was markedly lower than that in normal tissue (Fig. 1B). These findings implied that miR-34a may play a suppressive role in PCa progression.

miR-34a inhibits the PC3 cell cycle

To investigate the role of miR-34a in PCa progression, the activity of miR-34a was first detected using a dual-reporter gene assay. As shown in Fig. 2A, LacZ gene expression was obviously downregulated by miR-34a, suggesting that functional miR-34a was effectively expressed by the vector pAAVsc CB PI- miR-34a-Gluc, and it could regulate gene expression by targeting its binding site. Then, the cell cycle of PC3 cells overexpressing miR-34a was analyzed using flow cytometry (Fig. 2B). The data showed that miR-34a overexpression significantly increased PC3 cells in G_1 phase and decreased the cells in S phase (Fig. 2C). The data suggest that miR-34a overexpression can suppress PCa progression by inhibiting the cell cycle.

miR-34a suppresses PC3 cell viability and migration

In addition to its role in the cell cycle, the role of miR-34a in PC3 cell viability and migration was analyzed. As illustrated in Fig. 3A, the overexpression of miR-34a statistically inhibited PC3 cell viability. Next, a wound healing assay was used to detect cell migration, and the results indicated that miR-34a significantly inhibited cell migration in vitro (Fig. 3B, C). These findings further demonstrate that miR-34a can effectively inhibit PCa progression in vitro.

miR-34a downregulates target gene expression

To investigate the potential mechanism of miR-34a involved in PCa progression, the expression of the miR-34a target gene CCND1 was analyzed at the mRNA and protein levels in PC3 cells with or without miR-34a transfection. As shown in Fig. 4A–C, CCND1 expression was significantly decreased by miR-34a overexpression. These data suggested that miR-34a may inhibit PCa progression in vitro by downregulating CCND1 expression.

rAAV9 effectively and safely transduces mouse prostate and PCa cells in vivo

To investigate the role of miR-34a in PCa progression in vivo, the efficacy and safety profile of rAAV9 transduction was tested by intraprostatic and intratumoral injections. As shown in Fig. 5A, rAAV9 could effectively transduce mouse AP and DLP with GC numbers ranging from 5 to 10 GC/diploid genomes. Furthermore, mice bearing tumors of TRAMP-C2 cells (a PCa mouse cell line) were intratumorally injected with rAAV9 for 7 days, and the results showed that rAAV9 could effectively transduce tumor cells in vivo (Fig. 5B). In addition, the AST and ALT levels in mouse serum were measured, and no significant difference was observed between the PBS and rAAV9 groups (Fig. 5C). Overall, rAAV9 can effectively and safely transduce normal prostate and PCa cells in vivo, indicating that it is an appropriate tool for gene delivery.

rAAV9-miR-34a improves the survival of TRAMP mice by targeting downstream gene expression

After the intraprostatic injection, the weight of TRAMP mice was recorded every other week, and the animal weights in the miR-34a-treated group were markedly lower than those in the PBS group after 30 and 32 weeks of injection (Fig. 6A). Importantly, the survival rate of mice injected with miR-34a was obviously higher than that of mice injected with PBS (Fig. 6B). In particular, the median survival times for mice in the miR-34a and PBS groups were 307.5 and 220 days, respectively. Moreover, HE staining of prostate tissues revealed that miR-34a overexpression significantly reduced the neoplastic area in both AP and DLP (Fig. 7A, B). Furthermore, miR-34a overexpression in mouse prostates was confirmed by qPCR (Fig. 8A), and the protein expression level of its downstream target gene Ccnd1 was significantly decreased (Fig. 8B, C). These findings suggest that miR-34a overexpression can effectively inhibit PCa progression in vivo by targeting Ccnd1.

DISCUSSION

PCa is a major threat to male health worldwide, and its mortality is slowly decreasing in the USA; however, the incidence and death rate are increasing in developing countries (e.g.,

China). Recently, novel approaches and drugs were invented for the effective treatment of PCa; nevertheless, the efficacy of therapy and the rate of tumor recurrence still need to be improved. Studies on gene therapy for PCa were reported in the past two decades, and different genes were used as targets, including androgen receptor (AR), maspin, angiostatin, and endostatin [27–29], indicating great outlooks for the application of gene therapy.

miR-34a is a key regulator of PCa progression, and it has been found that miR-34a could be a tumor repressor. In addition, important oncogenes, such as cyclin D1 and AR, were reported to be directly downregulated by miR-34a, suggesting the crucial role of miR-34a in PCa [30, 31]. Moreover, our data also showed that miR-34a expression was decreased in the tumor tissue of TRAMP mice. Therefore, miR-34a was selected as a candidate target for repressing PCa progression.

Furthermore, the effects of miR-34a on the PCa cell cycle, viability and migration were comprehensively evaluated in vitro, and the results indicated that miR-34a can inhibit PCa development by targeting its downstream genes. CCND1 was deemed as a target of miR-34a [32, 33], and CCND1 is required for progression through the G1 phase of the cell cycle. At G1 phase, CCND1 is fastly synthesized and accumulates in the cell nuclei, and it is degraded at the S phase [34]. Thus, CCND1 downregulation by miR-34a inhibited PCa cell proliferation through suppressing cell cycle.

In this study, rAAV was selected as a tool for miR-34a delivery in prostate and PCa cells. Previously, studies on gene therapy of PCa utilized AAV serotype 2 as a vector for gene delivery [29]; however, the transduction efficacy of AAV2 in mouse prostate and PCa cells was relatively lower than that of other AAV serotypes [21]. To further investigate the efficacy and safety of rAAV transduction in vivo, particles of rAAV serotype 9 expressing EGFP were intraprostatically and intratumorally injected into the mouse prostate and xenografts, respectively. First, rAAV9 can effectively transduce mouse prostate, and the reporter gene showed long-term expression in prostate tissues (data not shown). Second, the tumor cells in the xenografts can be extensively transduced by rAAV9 after multiple site tumoral injection (the upper panel of Fig. 5B). Third, two indices of liver function, AST and ALT levels, in the PBS group were comparable in the rAAV9 injection group, partially indicating the safety of rAAV administration. Hence, the long-term expression, wide range of transduction and safety profile of rAAV9 shed light on the gene therapy of PCa using the rAAV system.

Although the weight and survival rate of TRAMP mice were accurately recorded after rAAV injection, this study did not show the tumor size of PCa due to the difficulties in measuring tumor size in the mouse abdomen. TRAMP mice can develop progressive forms of PCa with distant site metastasis and exhibit various forms of diseases from PIN to malignant neoplasia [22]. Therefore, TRAMP mice are an ideal model for studying the mechanism involved in PCa progression. The survival curve showed that miR-34a overexpression obviously extended the lifespan of TRAMP mice.

The role of miR-34a in inhibiting PCa progression was explored using histology analysis and western blotting. HE staining revealed that the degree of neoplasia was reduced in

both AP and DLP after miR-34a delivery. Importantly, the expression of downstream target genes of miR-34a was significantly decreased, suggesting that miR-34a may inhibit PCa progression by regulating the expression of its target genes.

Overall, miR-34a could be a potential therapeutic target for PCa treatment, and rAAV9 provides a useful tool for gene delivery. Our study developed a novel approach for the use of gene therapy to treat PCa, and it is an important supplement for the current therapeutics of PCa.

ACKNOWLEDGEMENTS

This study was supported by grants from National Natural Science Foundation of China (81702536, 82070784) to JA, grants from University of Massachusetts Medical School (an internal grant) and National Institutes of Health (R01NS076991-01,1P01AI100263-01, UG3 HL147367-01, 4P01HL131471-02, and R01HL097088) to GG, a grant from Science & Technology Department of Sichuan Province, China (2018HH0153) to JA, and a grant from 1.3.5 project for disciplines of excellence, West China Hospital, Sichuan University (ZYGD18011) to HL.

REFERENCES

1. Mattiuzzi C, Lippi G. Current cancer epidemiology. J Epidemiol Glob Health. 2019;9:217–22. [PubMed: 31854162]
2. Siegel RL, Miller KD, Jemal A. Cancer statistics, 2020. CA Cancer J Clin. 2020;70:7–30. [PubMed: 31912902]
3. Chipman JJ, Sanda MG, Dunn RL, Wei JT, Litwin MS, Crociani CM, et al. Measuring and predicting prostate cancer related quality of life changes using EPIC for clinical practice. J Urol. 2014;191:638–45. [PubMed: 24076307]
4. Jilg CA, Schultze-Seemann W, Drendel V, Vach W, Wieser G, Krauss T, et al. Detection of lymph node metastasis in patients with nodal prostate cancer relapse using (18)F/(11)C-choline positron emission tomography/computerized tomography. J Urol. 2014;192:103–10. [PubMed: 24518792]
5. Su HY, Chen ML, Hsieh PJ, Hsieh TS, Chao IM. Lung metastasis from prostate cancer revealed by 18F-FDG PET/CT without osseous metastasis on bone scan. Clin Nucl Med. 2016;41:392–3. [PubMed: 26859201]
6. Graham TJ, Box G, Tunariu N, Crespo M, Spinks TJ, Miranda S, et al. Preclinical evaluation of imaging biomarkers for prostate cancer bone metastasis and response to cabozantinib. J Natl Cancer Inst. 2014;106:dju033.
7. Yap TA, Smith AD, Ferraldeschi R, Al-Lazikani B, Workman P, de Bono JS. Drug discovery in advanced prostate cancer: translating biology into therapy. Nat Rev Drug Discov. 2016;15:699–718. [PubMed: 27444228]
8. Sluka P, Davis ID. Cell mates: paracrine and stromal targets for prostate cancer therapy. Nat Rev Urol. 2013;10:441–51. [PubMed: 23857181]
9. Olson BM, McNeel DG. Sipuleucel-T: immunotherapy for advanced prostate cancer. Open Access J Urol. 2011;3:49–60. [PubMed: 24198636]
10. Scher HI, Fizazi K, Saad F, Taplin ME, Sternberg CN, Miller K, et al. Increased survival with enzalutamide in prostate cancer after chemotherapy. N Engl J Med. 2012;367:1187–97. [PubMed: 22894553]
11. de Bono JS, Logothetis CJ, Molina A, Fizazi K, North S, Chu L, et al. Abiraterone and increased survival in metastatic prostate cancer. N Engl J Med. 2011;364:1995–2005. [PubMed: 21612468]
12. Chen CW, Fu M, Du ZH, Zhao F, Yang WW, Xu LH, et al. Long noncoding RNA MRPL23-AS1 promotes adenoid cystic carcinoma lung metastasis. Cancer Res. 2020;80:2273–2285. [PubMed: 32098781]
13. Wang L, Zheng C, Wu X, Zhang Y, Yan S, Ruan L, et al. Circ-SOX4 promotes non-small cell lung cancer progression by activating the Wnt/beta-catenin pathway. Mol Oncol. 2020;14:3253. [PubMed: 32112500]

14. Yuan Q, Yu H, Chen J, Song X, Sun L. Antitumor effect of miR-1294/pyruvate kinase M2 signaling cascade in osteosarcoma cells. Onco Targets Ther. 2020;13:1637–47. [PubMed: 32110059]
15. Akula SM, Ruvolo PP, McCubrey JA. TP53/miR-34a-associated signaling targets SERPINE1 expression in human pancreatic cancer. Aging. 2020;12:2777–97. [PubMed: 31986125]
16. Xie ZY, Wang FF, Xiao ZH, Liu SF, Tang SL, Lai YL. Overexpressing microRNA-34a overcomes ABCG2-mediated drug resistance to 5-FU in side population cells from colon cancer via suppressing DLL1. J Biochem. 2020;167:557–564.. [PubMed: 32044957]
17. Welponer H, Tsibulak I, Wieser V, Degasper C, Shivalingaiah G, Wenzel S, et al. The miR-34 family and its clinical significance in ovarian cancer. J Cancer. 2020;11:1446–56. [PubMed: 32047551]
18. Kashat M, Azzouz L, Sarkar SH, Kong D, Li Y, Sarkar FH. Inactivation of AR and Notch-1 signaling by miR-34a attenuates prostate cancer aggressiveness. Am J Transl Res. 2012;4:432–42. [PubMed: 23145211]
19. Ai J, Li J, Gessler DJ, Su Q, Wei Q, Li H, et al. Adeno-associated virus serotype rh.10 displays strong muscle tropism following intraperitoneal delivery. Sci Rep. 2017;7:40336. [PubMed: 28067312]
20. Bainbridge JW, Mehat MS, Sundaram V, Robbie SJ, Barker SE, Ripamonti C, et al. Long-term effect of gene therapy on Leber's congenital amaurosis. N Engl J Med. 2015;372:1887–97. [PubMed: 25938638]
21. Ai J, Wang D, Wei Q, Li H, Gao G. Adeno-associated virus serotype vectors efficiently transduce normal prostate tissue and prostate cancer cells. Eur Urol. 2016;69:179–81. [PubMed: 26526960]
22. Greenberg NM, DeMayo F, Finegold MJ, Medina D, Tilley WD, Aspinall JO, et al. Prostate cancer in a transgenic mouse. Proc Natl Acad Sci U S A. 1995;92:3439–43. [PubMed: 7724580]
23. Huss WJ, Maddison LA, Greenberg NM. Autochthonous mouse models for prostate cancer: past, present and future. Semin Cancer Biol. 2001;11:245–60. [PubMed: 11407949]
24. Sena-Esteves M, Gao G. Introducing genes into mammalian cells: viral vectors. Cold Spring Harb Protoc. 2020;2020:095513. [PubMed: 32457039]
25. Xie J, Ameres SL, Friedline R, Hung JH, Zhang Y, Xie Q, et al. Long-term, efficient inhibition of microRNA function in mice using rAAV vectors. Nat Methods. 2012;9:403–9. [PubMed: 22388288]
26. Ai J, Tai PWL, Lu Y, Li J, Ma H, Su Q, et al. Characterization of adenoviral transduction profile in prostate cancer cells and normal prostate tissue. Prostate. 2017;77:1265–70. [PubMed: 28726259]
27. Watanabe M, Nasu Y, Kashiwakura Y, Kusumi N, Tamayose K, Nagai A, et al. Adeno-associated virus 2-mediated intratumoral prostate cancer gene therapy: long-term maspin expression efficiently suppresses tumor growth. Hum Gene Ther. 2005;16:699–710. [PubMed: 15960601]
28. Sun A, Tang J, Terranova PF, Zhang X, Thrasher JB, Li B. Adeno-associated virus-delivered short hairpin-structured RNA for androgen receptor gene silencing induces tumor eradication of prostate cancer xenografts in nude mice: a pre-clinical study. Int J Cancer. 2010;126:764–74. [PubMed: 19642108]
29. Ponnazhagan S, Mahendra G, Kumar S, Shaw DR, Stockard CR, Grizzle WE, et al. Adeno-associated virus 2-mediated antiangiogenic cancer gene therapy: long-term efficacy of a vector encoding angiostatin and endostatin over vectors encoding a single factor. Cancer Res. 2004;64:1781–7. [PubMed: 14996740]
30. Fan C, Jia L, Zheng Y, Jin C, Liu Y, Liu H, et al. MiR-34a promotes osteogenic differentiation of human adipose-derived stem cells via the RBP2/NOTCH1/CYCLIN D1 coregulatory network. Stem Cell Rep. 2016;7:236–48.
31. Misso G, Di Martino MT, De Rosa G, Farooqi AA, Lombardi A, Campani V, et al. Mir-34: a new weapon against cancer? Mol Ther Nucleic Acids. 2014;3:e194.
32. Duan G, Zhang C, Xu C, Xu C, Zhang L, Zhang Y. Knockdown of MALAT1 inhibits osteosarcoma progression via regulating the miR34a/cyclin D1 axis. Int J Oncol. 2019;54:17–28. [PubMed: 30365098]
33. Liu Y, Gao S, Du Q, Zhao Q. Knockdown of long non-coding RNA metastasis associated lung adenocarcinoma transcript 1 inhibits the proliferation and migration of bladder cancer cells

by modulating the microRNA-34a/cyclin D1 axis. Int J Mol Med. 2019;43:547–56. [PubMed: 30387807]

34. Baldin V, Lukas J, Marcote MJ, Pagano M, Draetta G. Cyclin D1 is a nuclear protein required for cell cycle progression in G1. Genes Dev. 1993;7:812–21. [PubMed: 8491378]

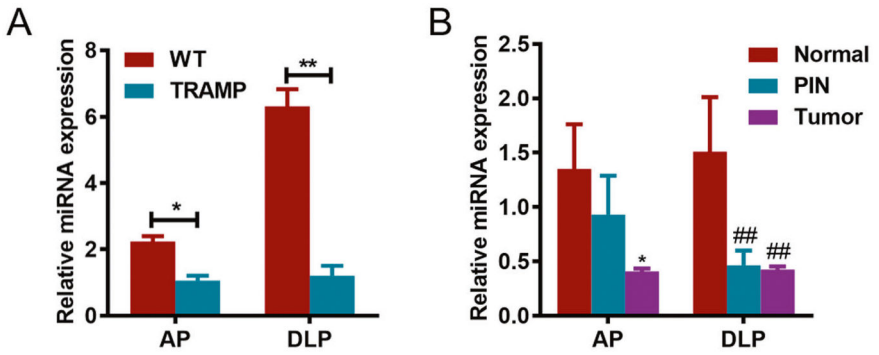

Fig. 1. miR-34a expression in prostate tumors of TRAMP mice.

A miR-34a expression was detected by qPCR in both AP and DLP of wild-type (WT) and TRAMP mice. **B** miR-34a expression was detected by qPCR in mouse prostates at stages of prostatic intraepithelial neoplasia (PIN) and tumors. AP anterior prostate, DLP dorsal lateral prostate, PIN prostatic intraepithelial neoplasia. $^{*}p < 0.05$; $^{**}p < 0.01$; $^{\#\#}p < 0.01$.

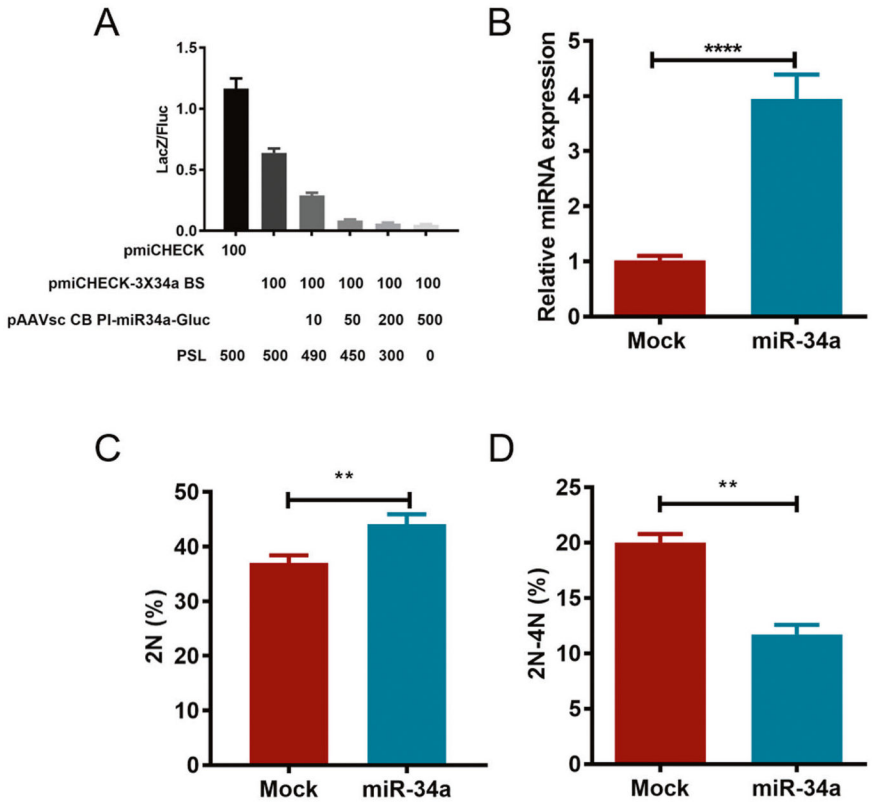

Fig. 2. miR-34a overexpression significantly inhibits the PC3 cell cycle in vitro.

A Dual-reporter assay was used to detect the activity of miR-34a. LacZ gene expression was reduced along with increased miR-34a expression (0, 10, 50, 200, and 500 ng of the pAAVsc CB PI-miR-34a-Gluc plasmid). The pmiCHECK plasmid was used as a positive control, and the sequence of the triple miR-34a binding site was inserted into the downstream region of the LacZ coding sequence (CDS) of pmiCHECK-3×34a BS. In total, 600-ng plasmids were transfected into cells of each group using the empty vector PSL plasmid. **B** The relative expression of miR-34a was detected by qPCR, and U6 was used as an internal control. The cell cycle was detected using flow cytometry, and the data were analyzed by Flow Jo software. The proportion of cells in G_1 (2N) and S (2–4N) phases are indicated in **C** and **D**, respectively. Fluc firefly luciferase. $^{**}p < 0.01$; $^{****}p < 0.0001$.

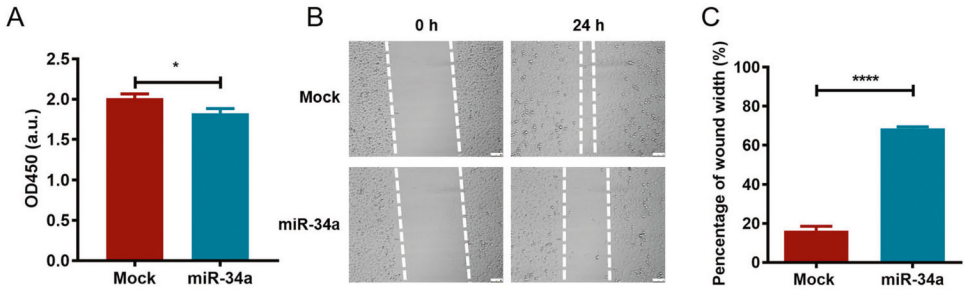

Fig. 3. miR-34a overexpression significantly suppresses PC3 cell viability and migration in vitro.

A PC3 cells were transfected with pAAVsc CB PI-miR-34a-Gluc for 48 h, and the CCK8 assay was used to evaluate cell viability by measuring the absorbance at 450 nm. **B** The wound healing assay was performed to investigate the effect of miR-34a on cell migration, and the wound width was recorded at 0 and 24 h using a microscope. **C** The wound width was statistically analyzed by ImageJ software. *$p < 0.05$; ****$p < 0.0001$.

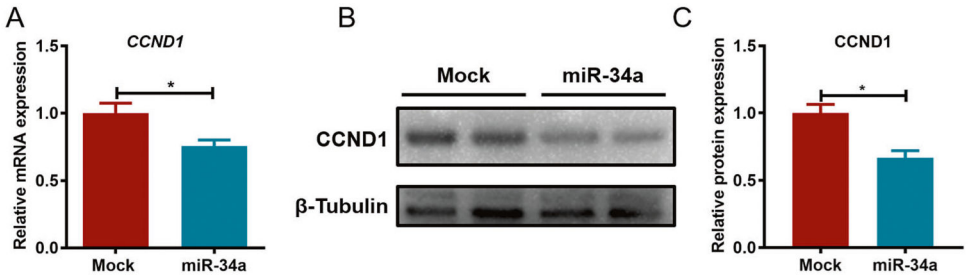

Fig. 4. miR-34a downregulates the expression of CCND1 in PC3 cells.

A CCND1 expression was detected using qPCR after miR-34a transfection, and β-actin was used as an internal control. **B** The expression of CCND1 was detected by western blotting, and β-tubulin was used as an internal control. **C** The band intensity of CCND1 was statistically analyzed by ImageJ software. $*p < 0.05$.

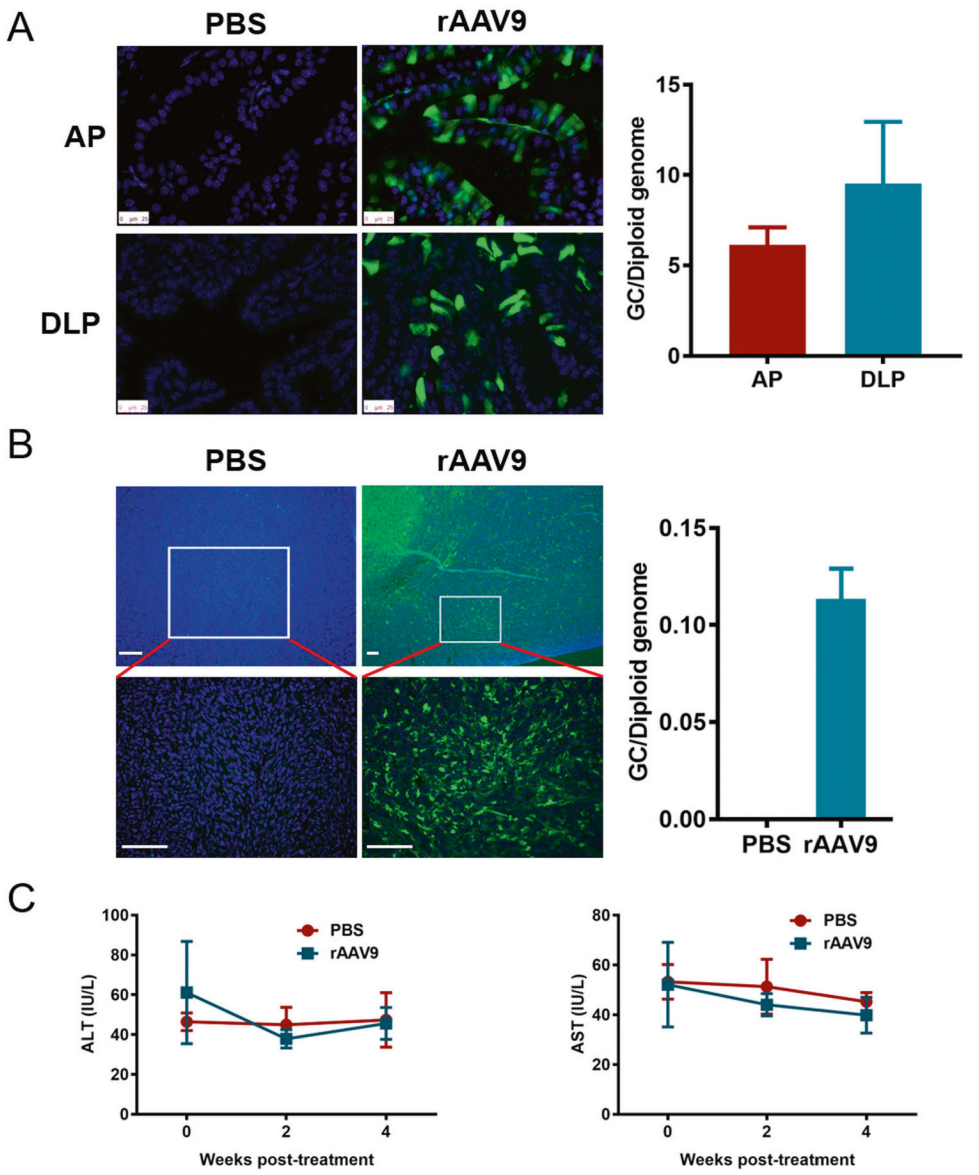

Fig. 5. rAAV9 effectively and safely transduces normal prostate and PCa cells in vivo.

A rAAV9-EGFP was injected into two lobes of the AP and two lobes of the DLP for 4 weeks. After cyrosectioning, EGFP fluorescence was observed using a fluorescence microscope. The AAV GC number in the prostate was detected using ddPCR. **B** Xenografts of TRAMP-C2 cells in C57 mice were intratumorally injected with rAAV9-EGFP for 7 days, and EGFP fluorescence was observed using a fluorescence microscope after cryosectioning at low and high magnification. The AAV GC number in tumor tissue was detected using ddPCR. **C** The ALT and AST levels were detected using sera from mice injected with rAAV9-EGFP. ALT alanine aminotransferase, AST aspartate aminotransferase.

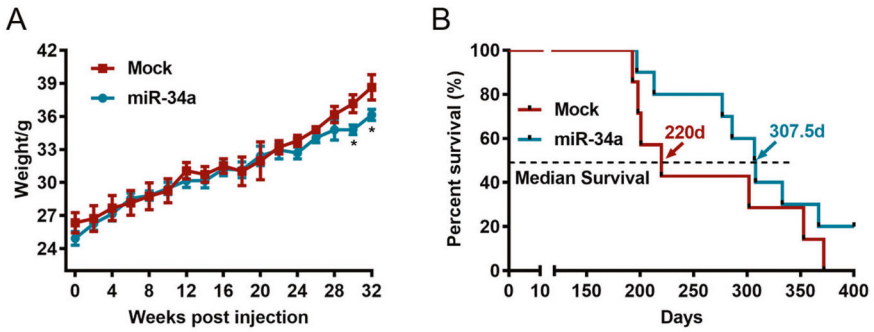

Fig. 6. miR-34a overexpression improves the survival of TRAMP mice.

A The weight of mice injected with rAAV9-miR-34a or PBS was recorded every other week. **B** The survival rates of mice injected with rAAV9-miR-34a or PBS. The median survival rate of mice in the miR-34a group (307.5 days) was obviously higher than that in the PBS group (220 days). *$p < 0.05$.

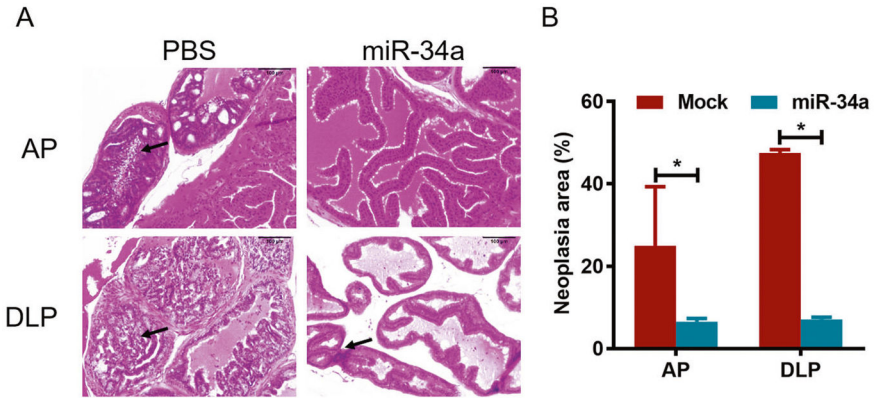

Fig. 7. miR-34a overexpression decreases the malignancy of PCa.

A Prostates of TRAMP mice injected with rAAV9-miR-34a or PBS were analyzed using HE staining, and the tumor cell number in the miR-34a group was lower than that in the PBS group. **B** The area of neoplasia in HE staining was calculated in both AP and DLP. *$p <$ 0.05.

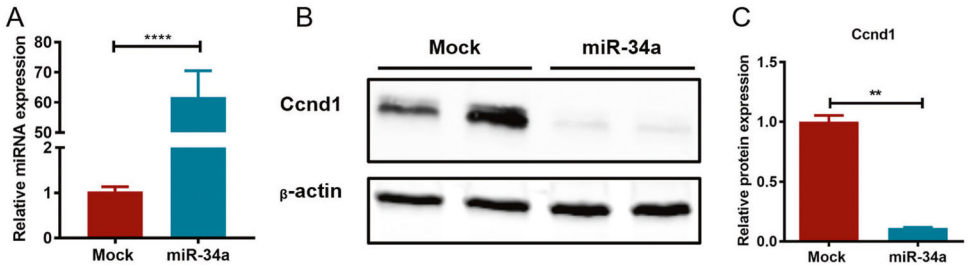

Fig. 8. miR-34a overexpression downregulates Ccnd1 gene expression in vivo.

A The expression of miR-34a in the prostates of TRAMP mice injected with rAAV9-miR-34a or PBS was detected using qPCR. **B** The protein expression of the miR-34a target gene Ccnd1 was detected using western blotting, and β-actin was used as an internal control. **C** The band intensities were calculated using ImageJ software. $^{**}p < 0.01$, $^{****}p < 0.0001$.

Table 1.

Primer information for qPCR.

	Forward (5′–3′)	Reverse (5′–3′)
CCND1	TGGAGCCCGTGAAAAAGAGC	TCTCCTTCATCTTAGAGGCCAC
TOP2A	ACCATTGCAGCCTGTAAATGA	GGGCGGAGCAAAATATGTTCC
CD44	CTGCCGCTTTGCAGGTGTA	CATTGTGGGCAAGGTGCTATT